

## 論文の内容の要旨

論文題目      Development of a magnetic marker for non-palpable  
breast cancer excision  
(乳腺非触知病変の局所切除のための  
磁性マーカーの開発)

氏      名      肖      穎怡

Breast cancer is the second leading cause of death for women nowadays. For early-stage breast cancer patient, breast conserving surgery removes the breast tumour while keeping as much normal breast as possible, which is a preferable treatment that can maintain high quality-of-life for patients. Most early-stage breast tumours are non-palpable. To perform the breast conserving surgery for non-palpable breast cancer, a localisation tool is required to aid surgeons make excision. Conventional localisation tools such as a hook wire cause high re-excision rate. Magnetic detection system is newly developed localisation method. However, existing magnetic marker have limited detectable distance, especially from the transverse direction where detection occurs.

In this research, we developed and evaluated novel magnetic markers numerically and experimentally for localization of non-palpable breast cancer, with the specifications of its size, detection performance and the coupled magnetic probe.

Firstly, magnetic properties and biocompatibility of materials are evaluated to determine the material selection. After calculation of baseline of magnetic susceptibility and residual magnetism required, and specify the biocompatibility restriction for such an implant device, four magnetic biocompatible material candidates, including three stainless steel, SUS 302, SUS 304 and SUS 316 and Nitinol NiTi, are chosen for further evaluation. Magnetic susceptibility and residual magnetism of selected materials are measured experimentally both with superconducting quantum interference device (SQUID) and with the handheld magnetic probe, with both results supporting the final decision of stainless steel (SUS) 304.

Numerical simulation system for evaluating the performance of magnetic markers is developed. The magnetic probe is simulated by dividing the permanent magnet into small elements, considering each element as a magnetic dipole and summing up the magnetic moment of all elements. Error between

measured magnetic field strength and simulation of the permanent magnet is 6.6%. This system is further used to evaluate the shape effect of magnetic markers. Magnetic markers are also divided into elements. Magnetisation of the magnetic marker can be calculated with the magnetic susceptibility of the material and the external magnetic field generated by the permanent magnet. Effect of pre-magnetisation applied on magnetic markers are evaluated. Magnetic susceptibility is improved with pre-magnetisation, according to the M-H curve of SUS 304. Four marker shapes, Y-, X-, Z- and Delta-shaped marker, are designed to increase the magnetic field strength in the perpendicular direction. Numerical detectable distance of each marker is evaluated, with and without pre-magnetisation. Delta-shaped marker has the longest detectable distance among four markers of 46 mm at the optimal separation angle. Using the cantilever model, force of marker at release exerts on tissue is evaluated. Delta-shaped and Z-shaped marker exerts the weakest pressure on breast tissue.






Prototypes are fabricated using SUS 304 wires. Shape distortion of prototypes after being pushed through 18-gauge injection needle in air is evaluated. Z-shaped marker have the least shape distortion, while Delta-shaped marker maintains the largest separation angle.

Performance of prototypes are evaluated experimentally. Magnetic characteristics of the magnetic markers are measured with the magnetic probe and compared with numerical simulation. Measured data shows high agreement with the numerical simulations, especially in the parallel orientation. In perpendicular direction, experimental detectable distance is the longest with X-shaped marker with 37 mm, and 33 mm for Y-shaped and Delta-shaped marker, with the application of transverse pre-magnetisation. Z-shaped marker has detectable distance of 27 mm in perpendicular direction, which does not meet the performance requirement.

Migration caused by magnetic attraction force is evaluated. No significant migration can be found with any marker prototype.

Experiment to evaluate the localisation accuracy of the markers in breast phantom is conducted. Volunteers are invited to localise markers in each phantom using the magnetic probe. 3D CT images of phantoms with the detected location marked with pin are taken. Localisation accuracy of the Delta-shaped marker is the highest, with average of 12.55 mm localisation error and standard deviation of 8.27. Meanwhile, all prototypes show average localisation error less than 15 mm, which is the required spatial resolution for the marker. No obvious agreement can be found between the detection error and the depth of the marker. No obvious agreement can be found between the detection error and the number of trials performed for each volunteer. Learning curve of the magnetic detection system is not significant. No strong learning curve can be found. In terms of structure stability, X-shaped marker prototypes collapse in agar phantom in 6/40 experiments, where the two wires separate completely. Delta-shaped marker shows its capability to maintain largest separation angle among the 4 marker shapes, with least variation in the separation angle. Y- and Z-shaped prototypes can maintain its stable structures. No strong agreement can be found between the number of repeated use and the separation angle variation of the magnetic markers.

Overall, Delta-shaped marker has the best performance, while Y-shaped marker also meets all requirements. With the focus on localisation of marker, Delta-shaped marker is taken into further investigation. Table below shows the overall comparison of all four marker shapes with the reference of a rod shape marker.

		reference	Y-shaped	X-shaped	Z-shaped	Delta-shaped
shape						
simulation	Optimal induced signal in perpendicular direction	$0.8 \mu T$	$1.6 \mu T$	$2.9 \mu T$	$3.6 \mu T$	$4.8 \mu T$
prototype	Distortion after injection	no	Large ( $14^\circ$ )	Large ( $22^\circ$ )	Small ( $5^\circ$ )	Large ( $25^\circ$ )
	Perpendicular detectable distance	N/A	33 mm	37 mm	27 mm	33 mm
	Significant Migration	no	no	no	no	no
	Accuracy of Localization ranking	N/A	3 (14.02 mm)	2 (13.52 mm)	4 (14.04mm)	1 (12.55mm)
	Average separation angle of prototypes	N/A	2 ( $34.3^\circ$ )	4 ( $25.3^\circ$ )	3 ( $35.6^\circ$ )	1 ( $38.3^\circ$ )